Bacteriophage cooperation suppresses CRISPR-Cas3 and Cas9 immunity

Adair L. Borges[1], Jenny Y. Zhang[1], MaryClare Rollins[2], Beatriz A. Osuna[1], Blake Wiedenheft[2], Joseph Bondy-Denomy[1,3*]

[1]Department of Microbiology and Immunology, University of California San Francisco, CA 94143, USA
[2] Department of Microbiology and Immunology, Montana State University, Bozeman, MT 59717, USA.
[3]Quantitative Biosciences Institute, University of California San Francisco, CA 94143, USA

*Correspondence: joseph.bondy-denomy@ucsf.edu

SUMMARY

Bacteria utilize CRISPR-Cas adaptive immune systems for protection from bacteriophages (phages), and some phages produce anti-CRISPR (Acr) proteins that inhibit immune function. Despite thorough mechanistic and structural information describing the mode-of-action for Acr proteins, how they are deployed by phages during infection is unknown. Here, we show that Acr production does not guarantee phage replication, but instead, CRISPR-Cas neutralization and phage infections fail when phage population numbers are too low. Failing infections can be rescued by kin phages acting as Acr producers, demonstrating that infections succeed if a sufficient Acr dose is contributed to a single cell by multiple phage genomes. The production of Acr proteins by phage genomes that fail to replicate leave the cell immunosuppressed, assisting other phages in the population. These observations apply generally to both Cas3 and Cas9-based adaptive immunity. This "cooperative phage" mechanism for CRISPR-Cas inhibition demonstrates inter-virus cooperation that may find parallels in other host-parasite interactions.

INTRODUCTION

Bacteria and the viruses that infect them (phages) are engaged in an ancient evolutionary arms race, which has resulted in the emergence of a diversity of CRISPR-Cas (clustered regularly interspaced short palindromic repeats and CRISPR-associated genes) adaptive immune systems (Koonin et al., 2017). CRISPR-Cas immunity is powered by the acquisition of small fragments of phage genomes into the bacterial CRISPR array, the subsequent transcription and processing of these arrays to generate small CRISPR RNAs, and the RNA-guided destruction of the phage genome (Barrangou et al., 2007; Brouns et al., 2008; Garneau et al., 2010; Levy et al., 2015). The destruction of foreign DNA by CRISPR-Cas has been shown to prevent the acquisition of plasmids, DNA from the environment, phage lytic replication, and prophage integration (Barrangou et al., 2007; Bikard et al., 2012; Cady et al., 2012; Edgar and Qimron, 2010; Garneau et al., 2010). In bacterial populations, these systems provide a fitness advantage to their host microbe during times of phage presence in the environment (van Houte et al., 2016; Westra et al., 2015).

To combat the potent action of RNA-guided CRISPR-Cas nucleases, phages have developed inhibitor proteins called anti-CRISPRs (Acrs). Acr proteins have been discovered that inhibit Type I-F (Bondy-Denomy et al., 2013; Pawluk et al., 2016b) and Type I-E (Pawluk et al., 2014) CRISPR-Cas3 systems, and also the Type II-A (Hynes et al., 2017; Rauch et al., 2017) and Type II-C (Pawluk et al., 2016a) CRISPR-Cas9 systems, across many distinct organisms (Borges et al., 2017; Pawluk et al., 2017). These proteins are likely ubiquitous in coevolving populations of bacteria and phages (Pawluk et al., 2017) and provide a significant replicative advantage to phages in the presence of CRISPR immunity (van Houte et al., 2016).

Anti-CRISPRs were first identified in phages that neutralize the *Pseudomonas aeruginosa* type I-F system (anti-CRISPR type I-F, AcrIF1-5)(Bondy-Denomy et al., 2013), and five more I-F anti-CRISPRs (AcrIF6-10) were subsequently identified in various mobile genetic elements (Pawluk et al., 2016b). The I-F Csy surveillance complex (also called Cascade) is comprised of four proteins (Csy1-4) and a *trans*-acting nuclease/helicase protein, Cas3 (Rollins et al., 2017; Wiedenheft et al., 2011). Anti-CRISPR proteins function by interacting directly with the Csy complex or Cas3, inhibiting DNA binding or cleavage by the immune system (Bondy-Denomy et al., 2015a). The structures of type I-F Acr proteins AcrIF1, AcrIF2, and AcrIF3 have been solved in complex with their target proteins, revealing mechanistically distinct inhibitors that bind tightly to their target Cas protein (Chowdhury et al., 2017; Guo et al., 2017; Maxwell et al., 2016; Wang et al., 2016). Together with the recent identification and characterization of proteins that inhibit Cas9, a common theme in Acr function has been revealed; all characterized Acr proteins are direct stoichiometric interactors of Cas proteins, blocking either phage DNA binding or cleavage (Dong et al., 2017; Harrington et al., 2017; Pawluk et al., 2016a; Rauch et al., 2017).

Despite a detailed mechanistic understanding, however, it is unknown how anti-CRISPR proteins are deployed by phages *in vivo*. During phage infection, we hypothesized that successful inhibition of CRISPR-Cas immunity by Acr proteins would be challenging, as all components of the *P. aeruginosa* immune system are expressed prior to phage infection (Bondy-Denomy et al., 2013; Cady et al., 2012). Where phage DNA cleavage has been assessed *in vivo*, it occurs in as little as 2 minutes (Garneau et al., 2010),

suggesting that CRISPR attack may outpace the ability of *de novo* Acr synthesis and action.

Here, we utilize the diverse array of AcrIF proteins encoded by phages to demonstrate that CRISPR-Cas inactivation is, in fact, a challenge, and that the sufficient concentration of Acr proteins necessary to inactivate CRISPR-Cas is contributed by multiple phage genomes. While initial phage infections may fail, due to the rapid action of the CRISPR-Cas system, immunosuppression can result due to the production of Acr proteins, which benefits phage in the community, leading to a population-level benefit for other phages. We propose that pathogens can contribute to the "remodeling" of their host cell via rapid protein production, even if the initial infecting genomes are cleared, opening the door for their clones.

RESULTS

Anti-CRISPR proteins are imperfect CRISPR-Cas inhibitors

We sought to utilize the diversity of *acr* genes encoded by phages infecting *P. aeruginosa* to determine the mechanism of CRISPR-Cas neutralization during infection. Five natural phages, each encoding a single *acrIF* gene, were selected to represent *acrIF1-IF4* and *acrIF7* (*acrIF5* does not exist as the sole *acrIF* gene on any phage, *acrIF6, F8-F10* are not encoded by this phage family). Three of these five phages exhibited reduced efficiency of plaquing (EOP) on *P. aeruginosa* strain wild-type (WT) PA14, possessing a type I-F CRISPR-Cas system, relative to a ΔCRISPR strain (Figure 1A, WT:pEmpty). Overexpression of a targeting crRNA (WT:pSp1) exacerbated anti-CRISPR inefficiency, limiting the replication of all anti-CRISPR phages by at least one order of magnitude. This suggests that anti-CRISPR proteins are unable to fully protect their associated phage genome.

To assess anti-CRISPR strength directly, an isogenic phage panel was generated by replacing the *acrIE3* gene of phage DMS3m with single *acrIF* genes *F1-F7* ($DMS3m_{acrIF1}$-$DMS3m_{acrIF7}$, Figure S1). WT PA14 (1 spacer targeting DMS3m, "1sp") and a laboratory evolved strain (5 spacers targeting DMS3m, "5sp") were challenged with the recombinant phages, revealing that all anti-CRISPRs are quantitatively imperfect during infection (Figure 1B). For phages encoding *acrIF1, F2, F3, F6* or *F7*, >90% of phage in the population failed to replicate (EOP=10^{-1}) when faced with 5 targeting spacers. *acrIF4*

and *F5* were very weak, with 99.0-99.99% of phages failing to replicate (EOP=10^{-2}-10^{-4}), depending on the CRISPR spacer content. We conclude that phages encoding *acrs* remain sensitive to CRISPR-Cas immunity, suggesting that anti-CRISPR deployment and action is an imperfect process.

Given the observation above of two groups of "strong" and "weak" Acr proteins, we selected a two representative AcrIF proteins for downstream experiments, with AcrIE3 as a negative control. AcrIF1 was selected as a model strong inhibitor, as its mechanism and binding affinity are known (Csy complex binding, K_D = 2.5 x 10^{-11} M)(Bondy-Denomy et al., 2015b; Chowdhury et al., 2017). In contrast, AcrIF4 is a weak inhibitor that also binds the Csy complex (Bondy-Denomy et al., 2015a), but with a significantly slower on-rate and faster off-rate compared to AcrIF1 (Figure 1C, Figure S2).

We next sought to assess the survival of bacterial cell populations over time, when infected with phages that must deploy Acr proteins, but where apparently only a minority of the population actually replicates. Phages were locked in the lytic cycle for the purpose of this experiment, by knocking out the *C repressor* gene (*gp1*) in DMS3m$_{acrIF1}$, DMS3m$_{acrIF4}$, and DMS3m$_{acrIE3}$. The virulent (vir) phages were used at varying concentrations to infect 5sp strains in liquid culture. In the presence of CRISPR immunity, phage replication and bacterial death only occurred at multiplicities of infection (MOI, input plaque forming units per colony forming unit) greater than 0.02 for the strong *acrIF1* (Figure 2A) and greater than an MOI of 2.0 (≥10^7 PFU) for the weak *acrIF4* (Figure 2B). Despite this high MOI-dependence, no selection or evolution of phage DMS3m$_{acrIF4}$ occurred throughout the experiment, as output phages remained as sensitive to CRISPR-Cas immunity as the input population (Figure S3). The phage encoding *acrIE3* was unable to replicate when faced with CRISPR immunity (Figure 2C), while in the absence of CRISPR, all phages replicated and cleared bacterial cultures similarly (Figure 2D-2F). These data demonstrate that while only a subset of the phage population may replicate, a critical phage concentration threshold exists for any replication to occur. The level of this threshold is inversely proportional to Acr strength, and this determines whether CRISPR-Cas immunity becomes inactivated at the population level.

Phage lytic replication requires Acr protein concentration thresholds be met

Concentration-dependent success of CRISPR-Cas neutralization during phage infection could be caused by an excess of phage DNA targets that overwhelm a cell by titrating Csy complexes away from other phages, or by the contribution of Acr proteins from multiple phage genomes in a single cell. To experimentally address these models, we genetically modified phages to render them non-replicative, thus allowing the independent titration of a subset of phages in the population. The immunity region from heteroimmune phage JBD30 (Figure S4A) was introduced into DMS3m phages, generating a hybrid phage, whose replication could be prevented by the overexpression of the JBD30 C repressor (*gp1*, Figure S4B). In the presence of the JBD30 C repressor, high doses of the hybrid phage did not replicate, confirming the efficacy of *gp1* overexpression (Figure S4C). This enabled the mixing of replicative and non-replicative phages, the latter acting as sacrificial genome and Acr donor, to assess the mechanism for the observed concentration dependency.

In the presence of non-replicating phages encoding *acrIF1*, and possessing the same five DNA target sequences, we observed a striking rescue effect, where this phage assisted in CRISPR-Cas neutralization, enabling DMS3m$_{acrIF1}$ (Figure 2G) and DMS3m$_{acrIF4}$ (Figure 2H) to replicate at input concentrations that are unsuccessful in the absence of the "helper phage". Although the input of helper phages was at a modest level (10^6 PFU, MOI = 0.2), this enabled the replicative phage to achieve an increase of phage titers by 4-5 orders of magnitude. However, this helping effect was not observed when the replicative phage did not encode an AcrIF protein (Figure 2I), or when the non-replicating phage produced *acrIE3* (Figure 2H-2I). Additionally, any potential lysogens formed by the DMS3m hybrid helper phage in this experiment would not have amplified the replicating phage, as these lysogens remain resistant to superinfection (Figure S4D). These data demonstrate that Csy complex titration by infecting phage genomes alone does not appear to be a significant "anti-CRISPR" factor in the outcome of phage replication or bacterial survival. Instead, the determinant of phage replicative success is the concentration of Acr proteins reached in single cells, which is achievable by Acr production from independent phage genomes. This suggests that multiple phage genomes can contribute to the "immunosuppression" of a single host by contributing separate doses of Acr protein, potentially explaining the observed concentration thresholds and inefficiencies observed in plaquing measurements.

Lysogeny requires Acr proteins contributed by transient intracellular genomes

All phages encoding Acr proteins that infect *P. aeruginosa* are naturally temperate, and can form lysogens by integrating into the bacterial genome. We therefore measured the impact of CRISPR and Acr proteins on lysogeny establishment during a single round of infection. While previous experiments examined cumulative phage replication in the lytic cycle over many hours, assaying lysogen formation over a short time frame is ideal for understanding the initial events that determine phage genome survival or cleavage. Additionally, lysogeny provides a direct readout for phage genome survival (i.e. an integrated prophage), while in lytic replication, phage survival leads to a dead cell that cannot be recovered. For these experiments, we selected the weak AcrIF4 protein as it provided the largest dynamic range of inefficiency in a single round of infection.

We generated derivatives of DMS3m$_{acrIF4}$ and DMS3m$_{acrIE3}$ marked with a gentamicin resistance cassette at the end of the genome, replacing a nonessential gene, *gp52*. This allowed the independent titration of two distinct and replicative phage populations and the selection and analysis of stable lysogens after the experiment. These phages were used to infect ΔCRISPR cells (0sp) for a time span less than a single round of infection (50 minutes, Figure S5), and the number of gentamicin resistant lysogens assessed. In the absence of CRISPR selection, a linear increase in the number of lysogens with increasing MOI was observed, over ~4 orders of magnitude (Figure 3A-3B, circles). In the presence of spacers targeting DMS3m (5sp), CRISPR reduced the efficiency of lysogeny (EOL, compared to 0sp) for the weak *acr* phage DMS3m$_{acrIF4}$, to such a degree that lysogeny was undetectable at low MOIs, and impaired by 100-1000-fold at higher MOIs (Figure 3A, triangles). DMS3m$_{acrIF4}$ demonstrated concentration dependence for successful lysogeny, with EOL values below or at the limit of detection for lower MOIs, increasing to EOL = 0.01 at higher MOIs (Figure 3C). Phage DMS3m$_{acrIE3}$ formed no lysogens at all input concentrations tested (Figure 3B, 3D), demonstrating the utility of an *acrIF* gene for lysogen establishment.

We hypothesized that if the concentration dependence for CRISPR neutralization during lysogeny could also be explained by phage cooperation, the “below-the-threshold” concentration of 10^3 LFU DMS3m$_{acrIF4}$ could be rescued by the addition of helper phages *in trans*. In accordance with this prediction, infection of the 5sp strain with a mixture of DMS3m$_{acrIF4}$ *gp52::gent* phages (10^3 LFU) and 10^7 PFU of unmarked helper phages

increased DMS3m$_{acrIF4}$ *gp52::gent* EOL dramatically. EOL increased by 2 orders of magnitude with helper phage DMS3m$_{acrIF1}$ and the DMS3m$_{acrIF4}$ helper phage increased EOL by 1 order of magnitude (Figure 3E). No such increase in lysogeny was observed for a phage without an *acrIF* gene, DMS3m$_{acrIE3}$ *gp52::gent* (Figure 3F). The addition of helper phages DMS3m$_{acrIE3}$, or an escaper phage DMS3m$_{acrIE3}$* had no effect on the EOL of the marked DMS3m$_{acrIF4}$ phage, demonstrating that the helper phage must be an Acr-producer.

To determine the outcome of this co-infection experiment we used the resulting lysogens as a genetic record of infection success for both the marked phage and the unmarked phage. Importantly, this family of Mu-like phage is capable of integrating randomly in the genome, enabling the formation of polylysogens(Bondy-Denomy et al., 2016). Thus, this allows us to distinguish whether the helper phage genome is still present as a prophage, in addition to the marked prophage which is selected for. All resulting lysogens tested (n=48) possessed only the marked prophage, with none possessing the helper prophage (Figure S6). This demonstrates that the transient presence of the helper phage genome (i.e. no lysogeny) in the same cell was sufficient to generate enough Acr protein to protect the marked phage, leading to the establishment of lysogens that would not exist if not for the helper (Figure 3E, compare “buffer” to “IF1”). The only time rare double lysogens were isolated, was when infecting with marked phage DMS3m$_{acrIE3}$ *gp52::gent*, and an unmarked DMS3m$_{acrIF1}$ helper phage (Figure 3F), since the prophage encoding *acrIE3* would be unable to neutralize CRISPR-Cas after lysogenic establishment and long-lasting protection from the helper prophage was required. Collectively, these data are consistent with a model where the production of Acr proteins from a transient phage genome prior to its cleavage generates an immunosuppressed cell that can be successfully parasitized by another phage upon re- or co-infection(s).

Stoichiometric inhibitors of Cas9 required bacteriophage cooperation

The intrinsic inefficiency of stoichiometric inhibitors likely manifests due to the rapid cleavage of a phage genome by CRISPR-Cas complexes, and the need to synthesize the Acr proteins *de novo* during infection. To determine whether this model generally applies to other stoichiometric inhibitors of bacterial immunity, we engineered a *P. aeruginosa* strain to express the Cas9 protein from *Streptococcus pyogenes* (SpyCas9) and engineered a DMS3m phage to express a previously identified stoichiometric

inhibitor of SpyCas9, AcrIIA4 (Dong et al., 2017; Rauch et al., 2017). In this entirely heterologous experiment, we observed the same inefficiency for a phage relying on an Acr protein. Spot-titration of phage lysates on a strain expressing a single guide RNA (sgRNA) targeting DMS3m decreased the titer of DMS3m$_{acrIE3}$ by many orders of magnitude, while DMS3m$_{acrIIA4}$ was protected (Figure 4A). However, quantification of the efficiency of plaquing again revealed that relying on an Acr protein for replication is imperfect, with an EOP = 0.4 (Figure 4B). In lytic replication infection experiments, DMS3m$_{acrIIA4}$ displayed concentration-dependent replication in the presence of CRISPR targeting (Figure 4C), while DMS3m$_{acrIE3}$ did not replicate in a concentration-dependent manner (Figure 4D). In the absence of CRISPR-Cas targeting, however, both phages replicated robustly (Figure 4E, 4F). To determine whether this concentration dependence to Cas9 inhibition was also a result if insufficient intracellular Acr dose, a non-replicative hybrid DMS3m$_{AcrIIA4}$ phage was generated and used as a helper during infection. Indeed, increased delivery of AcrIIA4 to cells allowed DMS3m$_{AcrIIA4}$ to replicated robustly from a concentration that was previously unsuccessful (Figure 4G), demonstrating phage cooperation to neutralize CRISPR-Cas9. Utilizing a single spacer sequence in this experiment, allowed for phage escape mutations to be more prevalent, and we observed that DMS3m$_{acrIE3}$ could also be helped by increased doses of AcrIIA4 from the phage population (Figure 4H), likely providing enough protection of that phage genome *in trans* to replicate and increase the frequency of escaper phages. This was not seen in previous experiments with 5 spacers targeting the phage, and may represent one example where Acr donations can be “cheated” upon by phages not contributing Acr proteins.

DISCUSSION

Here we demonstrate that the necessary intracellular concentration of an anti-immunity protein to achieve inactivation of cellular immunity depends on the relative strengths of both the inhibitor and the immunity pathway, which dictates the number of infecting viruses required in the population. We conclude that a single cell can become immunosuppressed by anti-immune protein contributions from independent infection events. In the absence of viral replication, these infection events serve to contribute to the inactivation of cellular immunity, thus enhancing the probability of successful infection events in the future (Figure 5). We expect that cooperation of this sort is

283 necessary when the immune process acts rapidly and irreversibly on the infecting viral
284 genome, as CRISPR-Cas immunity does.
285
286 The ability of phages to replicate in the lytic cycle or establish lysogens is impacted
287 dramatically by the number of phages in the population. To demonstrate phage-phage
288 cooperation for the deployment of Acr proteins, three distinct genetic strategies were
289 used, allowing the independent titration of phages encoding a defined Acr protein: i) non-
290 replicative Acr donor phages, ii) marked and unmarked phages to follow the fate of only
291 one phage, and iii) the prophage status of lysogens, as a genetic record of phage
292 success. As an experimental tool, restricting the replication of a subset of phages to
293 render them solely as Acr donors allowed the tracking of lytic replication of a “below-the-
294 threshold” concentration of replicative phages. In contrast, the prophage acquisition
295 experiment allows a more natural scenario, where all phages are replicative but an
296 antibiotic resistance marker allows one to track the outcome of one phage genotype,
297 starting at a concentration below its threshold for successful lysogeny. This
298 demonstrated that wild-type helper phages in the population contribute to cellular
299 immunosuppression, enabling the formation of lysogens that did not occur in their
300 absence. The presence of only a single, marked prophage in the bacterial genome
301 proves that the helper phage neither replicated (this would kill the cell), nor lysogenized
302 (prophage would be present), but had been present in the cell transiently.
303
304 The key result here is the observation that phages can remodel their host cell, even in
305 the absence of a replicating or integrated genome. It has long been known that
306 integrated prophages modulate host phenotypes via gene expression, including
307 superinfection exclusion, toxin production, and the production of Acr proteins (Bondy-
308 Denomy et al., 2013; Bondy-Denomy and Davidson, 2014; Bondy-Denomy et al., 2016;
309 Waldor and Mekalanos, 1996; Weigle and Delbruck, 1951). Although less commonly
310 described, there is also precedent for lytic phages to impact an interaction with other
311 phages during replication. The Imm protein produced by the phage T4 prevents other
312 phages in the environment from infecting the cell that one phage is currently replicating
313 within (Lu and Henning, 1989). This has been attributed to preventing superinfection and
314 the potential disruption of the carefully timed phage replication cycle. This supports a
315 conclusion that co- and/or re-infections are a common occurrence in nature. However,
316 here, we propose new model of phage-induced host remodeling; that transient, cleared

genomes produce proteins that could enable future infections, by inactivating defense. This phenomenon would be evolutionarily advantageous in a clonal phage population, where all are providing Acr proteins to neutralize CRISPR, and as shown in Figure 2I, a phage not making an AcrIF protein was unable to “cheat” despite the presence of helper phages in the population.

A distinct, but notable observation from this work is that not all Acr proteins operate at full strength, as AcrIF4 and AcrIF5 provide weak protection to their phage genome. However, encoding these genes still provides a significant advantage to the phage, compared to lacking them entirely. Because the mechanism of action for AcrIF5 is still unknown, we focused on AcrIF4, demonstrating that its affinity for the Csy complex is orders of magnitude lower than stronger Acr proteins like AcrIF1. At present, however, we lack an explanation for why a weak Acr protein would be utilized by phages if stronger variants are available. AcrIF1 was selected as a model strong Acr protein because of its comparable mechanism of action to AcrIF4 (i.e. Csy complex binding). We consider AcrIF1 to be representative for other strong Acr proteins (AcrIF2, F3, F6, F7) as phages encoding them had similar efficiencies of plaquing, and we therefore expect similar threshold concentrations. Going forward, we speculate that the strongest Acr proteins would be enzymatic in nature, allowing rapid and efficient inactivation of CRISPR complexes in a sub-stoichiometric manner, although no such Acr mechanism has been discovered. While not an enzyme, the recent demonstration of the AcrIIC3 protein inactivating two Cas9 proteins at the same time would likely be a more efficient path towards CRISPR neutralization (Harrington et al., 2017).

The challenge of neutralizing a pre-expressed CRISPR-Cas system likely explains why stoichiometric inhibitors like Acr proteins are imperfect, and phages relying on them are partially targeted by CRISPR. The sacrificial, population-level aspect of CRISPR inhibition is reminiscent of the manifestations of CRISPR adaptation in populations of bacterial cells. The majority of infected naïve host cells die, before a clone with a new spacer emerges (Barrangou et al., 2007; Hynes et al., 2014). In the case of anti-immunity, many phages die in order to inhibit CRISPR on a single cell level, and this must happen at sufficient frequency within an ecosystem for phage to prevail. We suspect that this mechanism of cellular immunosuppression and inter-parasite cooperation may have parallels in other host-pathogen interactions, where concentration

dependence manifests at predictable levels due the strengths of immune and anti-immune processes.

SUPPLEMENTAL INFORMATION

Figures S1-S6 are provided separately.

AUTHOR CONTRIBUTIONS

A.L.B. and J.B.D. designed experiments and wrote the manuscript. A.L.B. engineered phage variants and conducted all experiments with the exception of binding affinity measurements. J.Y.Z. assisted with experimental design and execution, phage engineering, and data collection. B.A.O. built the Cas9 strain in *Pseudomonas aeruginosa.* J.B.D. supervised experiments. M.R. conducted Acr binding affinity measurements under the supervision of B.W. All authors contributed to data analysis and edited the manuscript.

ACKNOWLEDGEMENTS

The Bondy-Denomy lab was supported by the University of California San Francisco Program for Breakthrough in Biomedical Research, funded in part by the Sandler Foundation, and an NIH Office of the Director Early Independence Award (DP5-OD021344). Research in the Wiedenheft lab is supported by the National Institutes of Health (P20GM103500, P30GM110732, R01GM110270, R01GM108888 and R21 AI130670), the National Science Foundation EPSCoR (EPS-110134), the M. J. Murdock Charitable Trust, a young investigator award from Amgen, and the Montana State University Agricultural Experimental Station (USDA NIFA).

REFERENCES

Barrangou, R., Fremaux, C., Deveau, H., Richards, M., Boyaval, P., Moineau, S., Romero, D.A., and Horvath, P. (2007). CRISPR provides acquired resistance against viruses in prokaryotes. Science *315*, 1709–1712.

Bikard, D., Hatoum-Aslan, A., Mucida, D., and Marraffini, L.A. (2012). CRISPR interference can prevent natural transformation and virulence acquisition during in vivo bacterial infection. Cell Host Microbe *12*, 177–186.

Bondy-Denomy, J., Pawluk, A., Maxwell, K.L., and Davidson, A.R. (2013). Bacteriophage genes that inactivate the CRISPR/Cas bacterial immune system. Nature *493*, 429–432.

Bondy-Denomy, J., and Davidson, A.R. (2014). When a virus is not a parasite: the beneficial effects of prophages on bacterial fitness. J Microbiol *52*, 235–242.

Bondy-Denomy, J., Garcia, B., Strum, S., Du, M., Rollins, M.F., Hidalgo-Reyes, Y., Wiedenheft, B., Maxwell, K.L., and Davidson, A.R. (2015a). Multiple mechanisms for CRISPR-Cas inhibition by anti-CRISPR proteins. Nature *526*, 136–139.

Bondy-Denomy, J., Garcia, B., Strum, S., Du, M., Rollins, M.F., Hidalgo-Reyes, Y., Wiedenheft, B., Maxwell, K.L., and Davidson, A.R. (2015b). Multiple mechanisms for CRISPR-Cas inhibition by anti-CRISPR proteins. Nature *526*, 136–139.

Bondy-Denomy, J., Qian, J., Westra, E.R., Buckling, A., Guttman, D.S., Davidson, A.R., and Maxwell, K.L. (2016). Prophages mediate defense against phage infection through diverse mechanisms. The ISME Journal *10*, 2854–2866.

Borges, A.L., Davidson, A.R., and Bondy-Denomy, J. (2017). The Discovery, Mechanisms, and Evolutionary Impact of Anti-CRISPRs. Annual Review of Virology *4*, annurev–virology–101416–041616.

Brouns, S.J.J., Jore, M.M., Lundgren, M., Westra, E.R., Slijkhuis, R.J.H., Snijders, A.P.L., Dickman, M.J., Makarova, K.S., Koonin, E.V., and van der Oost, J. (2008). Small CRISPR RNAs guide antiviral defense in prokaryotes. Science *321*, 960–964.

Cady, K.C., Bondy-Denomy, J., Heussler, G.E., Davidson, A.R., and O'Toole, G.A. (2012). The CRISPR/Cas adaptive immune system of Pseudomonas aeruginosa mediates resistance to naturally occurring and engineered phages. *194*, 5728–5738.

Chowdhury, S., Carter, J., Rollins, M.F., Golden, S.M., Jackson, R.N., Hoffmann, C., Nosaka, L., Bondy-Denomy, J., Maxwell, K.L., Davidson, A.R., et al. (2017). Structure Reveals Mechanisms of Viral Suppressors that Intercept a CRISPR RNA-Guided Surveillance Complex. Cell *169*, 47–57.e11.

Dong, D., Guo, M., Wang, S., Zhu, Y., Wang, S., Xiong, Z., Yang, J., Xu, Z., and Huang, Z. (2017). Structural basis of CRISPR-SpyCas9 inhibition by an anti-CRISPR protein. Nature.

Edgar, R., and Qimron, U. (2010). The Escherichia coli CRISPR system protects from λ lysogenization, lysogens, and prophage induction. J. Bacteriol. *192*, 6291–6294.

Garneau, J.E., Dupuis, M.-È., Villion, M., Romero, D.A., Barrangou, R., Boyaval, P., Fremaux, C., Horvath, P., Magadán, A.H., and Moineau, S. (2010). The CRISPR/Cas bacterial immune system cleaves bacteriophage and plasmid DNA. Nature *468*, 67–71.

Guo, T.W., Bartesaghi, A., Yang, H., Falconieri, V., Rao, P., Merk, A., Eng, E.T., Raczkowski, A.M., Fox, T., Earl, L.A., et al. (2017). Cryo-EM Structures Reveal Mechanism and Inhibition of DNA Targeting by a CRISPR-Cas Surveillance Complex. Cell *171*, 414–426.e12.

Harrington, L.B., Doxzen, K.W., Ma, E., Liu, J.-J., Knott, G.J., Edraki, A., Garcia, B., Amrani, N., Chen, J.S., Cofsky, J.C., et al. (2017). A Broad-Spectrum Inhibitor of CRISPR-Cas9. Cell.

Hynes, A.P., Rousseau, G.M., Lemay, M.-L., Horvath, P., Romero, D.A., Fremaux, C., and Moineau, S. (2017). An anti-CRISPR from a virulent streptococcal phage inhibits Streptococcus pyogenes Cas9. Nature Microbiology *315*, 1.

Hynes, A.P., Villion, M., and Moineau, S. (2014). Adaptation in bacterial CRISPR-Cas immunity can be driven by defective phages. Nature Communications *5*, 4399.

Koonin, E.V., Makarova, K.S., and Wolf, Y.I. (2017). Evolutionary Genomics of Defense Systems in Archaea and Bacteria. Annu Rev Microbiol *71*, annurev–micro–090816–093830.

Levy, A., Goren, M.G., Yosef, I., Auster, O., Manor, M., Amitai, G., Edgar, R., Qimron, U., and Sorek, R. (2015). CRISPR adaptation biases explain preference for acquisition of foreign DNA. *520*, 505–510.

Lu, M.J., and Henning, U. (1989). The immunity (imm) gene of Escherichia coli bacteriophage T4. Journal of Virology *63*, 3472–3478.

Maxwell, K.L., Garcia, B., Bondy-Denomy, J., Bona, D., Hidalgo-Reyes, Y., and Davidson, A.R. (2016). The solution structure of an anti-CRISPR protein. Nature Communications *7*, 13134.

Pawluk, A., Amrani, N., Zhang, Y., Garcia, B., Hidalgo-Reyes, Y., Lee, J., Edraki, A., Shah, M., Sontheimer, E.J., Maxwell, K.L., et al. (2016a). Naturally Occurring Off-Switches for CRISPR-Cas9. Cell *167*, 1829–1838.e1829.

Pawluk, A., Bondy-Denomy, J., Cheung, V.H.W., Maxwell, K.L., and Davidson, A.R. (2014). A new group of phage anti-CRISPR genes inhibits the type I-E CRISPR-Cas system of Pseudomonas aeruginosa. mBio *5*, e00896–e00896–14.

Pawluk, A., Davidson, A.R., and Maxwell, K.L. (2017). Anti-CRISPR: discovery, mechanism and function. Nat Rev Micro *1*, nrmicro.2017.120.

Pawluk, A., Staals, R.H.J., Taylor, C., Watson, B.N.J., Saha, S., Fineran, P.C., Maxwell, K.L., and Davidson, A.R. (2016b). Inactivation of CRISPR-Cas systems by anti-CRISPR proteins in diverse bacterial species. Nature Microbiology *1*, 1–6.

Rauch, B.J., Silvis, M.R., Hultquist, J.F., Waters, C.S., McGregor, M.J., Krogan, N.J.,

and Bondy-Denomy, J. (2017). Inhibition of CRISPR-Cas9 with Bacteriophage Proteins. Cell *168*, 150–158.e10.

Rollins, M.F., Chowdhury, S., Carter, J., Golden, S.M., Wilkinson, R.A., Bondy-Denomy, J., Lander, G.C., and Wiedenheft, B. (2017). Cas1 and the Csy complex are opposing regulators of Cas2/3 nuclease activity. Proceedings of the National Academy of Sciences *23*, 201616395–E5121.

van Houte, S., Ekroth, A.K.E., Broniewski, J.M., Chabas, H., Ben Ashby, Bondy-Denomy, J., Gandon, S., Boots, M., Paterson, S., Buckling, A., et al. (2016). The diversity-generating benefits of a prokaryotic adaptive immune system. Nature *532*, 385–388.

Waldor, M.K., and Mekalanos, J.J. (1996). Lysogenic conversion by a filamentous phage encoding cholera toxin. Science *272*, 1910–1914.

Wang, X., Yao, D., Xu, J.-G., Li, A.-R., Xu, J., Fu, P., Zhou, Y., and Zhu, Y. (2016). Structural basis of Cas3 inhibition by the bacteriophage protein AcrF3. Nat. Struct. Mol. Biol. *23*, 868–870.

Weigle, J.J., and Delbruck, M. (1951). Mutual exclusion between an infecting phage and a carried phage. J. Bacteriol. *62*, 301–318.

Westra, E.R., van Houte, S., Oyesiku-Blakemore, S., Makin, B., Broniewski, J.M., Best, A., Bondy-Denomy, J., Davidson, A., Boots, M., and Buckling, A. (2015). Parasite Exposure Drives Selective Evolution of Constitutive versus Inducible Defense. Curr. Biol. *25*, 1043–1049.

Wiedenheft, B., van Duijn, E., Bultema, J.B., Bultema, J., Waghmare, S.P., Waghmare, S., Zhou, K., Barendregt, A., Westphal, W., Heck, A.J.R., et al. (2011). RNA-guided complex from a bacterial immune system enhances target recognition through seed sequence interactions. Proceedings of the National Academy of Sciences *108*, 10092–10097.

FIGURE LEGENDS

Figure 1. Anti-CRISPRs are imperfect CRISPR-Cas inhibitors

(A) Efficiency of plaquing (EOP) of 5 related phages bearing distinct *acrIF* genes (JBD30$_{acrIF1}$, MP29$_{acrIF2}$, JBD88a$_{acrIF3}$, JBD24$_{acrIF4}$, LPB1$_{acrIF7}$) on *Pseudomonas aeruginosa* strain PA14. Plaque forming units (PFUs) were quantified on wild-type PA14 with 1-2 natural targeting spacers (WT + pEmpty) or on PA14 overexpressing 1 targeting spacer (WT + pSp1), then normalized to the number of PFUs measured on a non-targeting PA14 derivative (0sp). Data are represented as the mean of 3 biological replicates +/- SD.

(B) EOP of isogenic DMS3m phages with *acrIF1-7* or *acrIE3* in the DMS3m *acr* locus. EOP was calculated as PFU counts measured on WT PA14 with 1 targeting spacer (1sp) or a laboratory evolved PA14 derivative with 5 targeting spacers (5sp) normalized to PFU counts measured on non-targeting PA14 (0sp). Data are represented as the mean of 3 biological replicates +/- SD. ND, not detectable.

(C) Plot of association (Ka) and dissociation (Kd) rates for AcrIF1 (data adapted from Chowdhury et al. 2017) and AcrIF4 binding the PA14 Csy complex. See Figure S2 for SPR AcrIF4 sensogram.

Figure 2. Anti-CRISPR success requires cooperative infections during lytic growth

(A-F) 12 h growth curves of *P. aeruginosa* strain PA14 with 5 targeting spacers (+CRISPR, panels **A-C**) or no CRISPR-Cas function (ΔCRISPR, **D-F**) infected with virulent variants of DMS3m$_{acrIF1}$, DMS3m$_{acrIF4}$, or DMS3m$_{acrIE3}$ at multiplicity of infection (MOI) increasing in 10-fold steps from $2x10^{-5}$ to $2x10^{1}$ (rainbow colors) or uninfected (black). Phage were harvested after 24 hours and quantified as PFUs on PA14 0sp (horizontal bars). Colors correspond to the MOI legend and growth curves. OD600 and phage output are represented as the mean of 3 biological replicates +/- SD. ND, not detectable.

(G-I) Replication of virulent DMS3m$_{acr}$ phages (target phage) in the presence of 10^{6} PFU (MOI 0.2) hybrid phage (donor) in PA14 with 5 targeting spacers expressing the JBD30 C-repressor. Phages were harvested after 24 hours of co-culture and DMS3m$_{acr}$ phage PFUs were quantified on PA14 0sp expressing the JBD30 C repressor. Phage output is represented as the mean of 3 biological replicates +/- SD. ND, not detectable.

Figure 3. Immunosuppression facilitates acquisition of a marked prophage

(**A,B**) Acquisition of marked DMS3m$_{acrIF4}$ or DMS3m$_{acrIE3}$ prophage by PA14 with 0 spacers (0 sp, circles) or 5 targeting spacers (5 sp, triangles). This experiment was performed in biological triplicate, and individual replicate values are displayed. LoD, limit of detection.

(**C,D**) Efficiency of lysogeny (EOL) of DMS3m$_{acrIF4\ gp52::gentR}$ and DMS3m$_{acrIE3\ gp52::gentR}$ in the presence of CRISPR targeting. EOL was calculated by dividing the output lysogens forming units (LFUs) from the strain with 5 targeting spacers (5sp) to the number of LFUs in PA14 with 0 targeting spacers (0sp). Data are represented as the mean of 3 biological replicates +/- SD. ND, not detectable.

(**E,F**) EOL of 10^3 LFUs of DMS3m$_{acrIF4\ gp52::gentR}$ and DMS3m$_{acrIE3\ gp52::gentR}$ in the presence of 10^7 PFU of the indicated DMS3m$_{acr}$ phage. Data are represented as the mean of 3 biological replicates +/- SD. ND, not detectable. See Figure S6 for lysogen genetic analysis.

Figure 4. Cas9 anti-CRISPR AcrIIA4 requires cooperative infection to neutralize Type II-A CRISPR immunity

(A) 10-fold serial dilutions of DMS3m$_{acrIE3}$ or DMS3m$_{acrIIA4}$ plated on a lawn of *Pseudomonas aeruginosa* strain PAO1 expressing *Streptococcus pyogenes* Type II-A Cas9 (PAO1::SpyCas9) and single guide RNA (+ sgRNA) or non-targeting control (+ vector).

(B) Efficiency of plaquing of DMS3m$_{acrIIA4}$ and DMS3m$_{acrIE3}$ was calculated by normalizing PFU counts on a targeting strain of PAO1::SpyCas9 (+sgRNA) to PFU counts on a non-targeting strain of PAO1::SpyCas9 (+vector). Data are represented as the mean of 3 biological replicates +/- SD. ND, not detectable.

(C-F) 12 hour growth curves of PAO1::spyCas9 expressing a targeting sgRNA (+ sgRNA, panels **C-D**) or a non-targeting vector control (+vector, E-F) that were infected with virulent DMS3m$_{acrIIA4}$ or DMS3m$_{acrIE3}$ at multiplicities of infection (MOI, rainbow colors) from $2x10^{-5}$ to $2x10^{-2}$. Growth curves of uninfected cells are shown in black. Phage were harvested after 24 hours and PFUs quantified on PAO1::SpyCas9 + vector (horizontal bars). OD600 and phage output are represented as the mean of 3 biological replicates +/- SD.

(G-H) Replication of virulent DMS3m$_{acr}$ phages (target phage) in the presence of 10^7 PFU (MOI 2) hybrid phage (donor) in PAO1::SpyCas9 + sgRNA expressing the JBD30 C-repressor. Phages were harvested after 24 hours and DMS3m$_{acr}$ phage PFUs quantified on PAO1::SpyCas9 + vector expressing the JBD30 C repressor. Phage output is represented as the mean of 3 biological replicates +/- SD. ND, not detectable.

Figure 5. Phage cooperation to suppress CRISPR-Cas immunity

Left: Failed infections generate an immunosuppressed cell. While the phage genome may be cleaved (dashed red line), Acr protein (small cyan circles) will be produced, binding to some CRISPR-Cas complexes (larger purple structures, with crRNA). *Right:* At low parasite density, it is unlikely the cell will be re-infected and the host will survive. As high parasite density, the likelihood that the immunosuppressed cell with be re-

infected is higher. Co- or re-infection will lead to successful parasite replication and amplification of the infectious population.

SUPPLEMENTAL FIGURE LEGENDS

Figure S1. Engineering DMS3m$_{acr}$ phages

(A) Schematic of two *acr* locus architectures used to generate an isogenic family of DMS3m$_{acr}$ phages.

(B) Efficiency of plaquing (EOP) of DMS3m$_{acrIF1}$ with natural or synthetic locus architecture on PA14 with 1 or 5 targeting spacers (1sp and 5 sp). Data are represented as the mean of 3 biological replicates +/- SD.

(C) Table of DMS3m$_{acr}$ phage genotype and locus architecture, as well as the original source of the *acr* gene and the corresponding accession number of the Acr protein.

Figure S2. Sensograms of AcrIF4 and AcrIF1 binding the Csy complex

(A) Sensogram showing real-time binding of increasing concentrations of free AcrIF4 (1.85 nM, 55.6 nM, 167 nM, 500 nM, 1.5 μM) to immobilized Csy complex. A model describing Langmuir binding (black line) was fit to the data to calculate binding constants (Ka, Kd, and KD; boxed inset).

(B) Sensogram showing real-time binding of increasing concentrations of free AcrIF1 (1.85 nM, 55.6nM, 167 nM, 500 nM, 1.5 μM) to immobilized Csy complex. A model describing binding at a 2:1 stoichiometry of free analyte:immobilized ligand (black line) was fit to the data to calculate binding constants (Ka1, Ka2, Kd1, Kd2, and KD1, KD2; boxed inset) (Chowdhury and et al. 2017).

Figure S3. Output phages from Figure 1B are CRISPR sensitive

Efficiency of plaquing (EOP) of the original stock of virulent DMS3macr$_{IF4}$ (input) on PA14 5 sp compared to EOP of DMS3m$_{acrIF4}$ harvested from high MOI infections (MOI 2, MOI 20 output) from figure 2B. Data are represented as the mean of 3 biological replicates +/- SD.

Figure S4. Generating and validating Hybrid$_{acr}$ phages

(A) 10-fold serial dilutions of DMS3m$_{acrIE3}$ and JBD30$_{acrIF1}$ spotted on lawns of non-targeting (0sp) *Pseudomonas aeruginosa* PA14 expressing the DMS3m C repressor (*gp1-DMS3m*), the JBD30 C repressor (*gp1-JBD30*) or a vector control.

(B) 10-fold serial dilutions of hybrid DMS3m$_{acrIE3\ gp1\text{-}JBD30}$ plated on lawns of non-targeting (0sp) *Pseudomonas aeruginosa* PA14 expressing the DMS3m C repressor (*gp1-DMS3m*), the JBD30 C repressor (*gp1-JBD30*), or a spacer which uniquely targets JBD30 (2sp17).

(C) Hybrid phage (Hybrid$_{acrIF1}$ or Hybrid$_{acrIE3}$) harvested from infections of PA14 5sp expressing the JBD30 C repressor from experiments shown in Figure 2G-I. Hybrid PFUs were quantified on the 0sp PA14 strain. Data are represented as the mean of 3 biological replicates +/- SD.

(D) 10-fold serial dilutions of JBD30$_{acrIF1}$ or virulent DMS3m$_{acrIE3}$ spotted on lawns of PA14 Δ*csy3* or PA14 Δ*csy3* lysogenized with Hybrid$_{acrIE3}$ or Hybrid$_{acrIF1}$. Despite being heteroimmune with respect to DMS3, the DMS3 phage is unable to replicate well on this lysogens due to other superinfection exclusion properties of DMS3.

Figure S5. Timecourse of lysogen formation

Time course of acquisition of gentamicin-resistance marked DMS3m$_{acrIFI\ gp52::gentR}$ prophage by a non-targeting (0 sp) strain of PA14, labeled with estimates of each infectious cycle (Rounds 1-3). Data are represented as the mean of 3 biological replicates +/- SD.

Figure S6. Prophage content of lysogens from Figure 3E-F

(A) 10-fold serial dilutions of supernatant harvested from overnight cultures of lysogens from Figure 3E (1-48) and 3F (49-51), spotted on a non-targeting (0 sp) strain of PA14. A faint clearing corresponds to induction of the gentamicin marked phage, while strong plaquing (i.e. 50, 51) reflects the presence of the gentamicin marked phage and the helper phage.

(**B**) PCR of genomic DNA harvested from harvested from overnight cultures of lysogens from Figure 3E (1-48) and 3F (49-51) amplified with primers targeting *gp52-DMS3m* (top) or the gentamicin resistance cassette used to replace *gp52* in *DMS3m*$_{acr\ gp52::gentR}$ derivatives (bottom).

METHODS

Strains and growth conditions

Pseudomonas aeruginosa strains (UCBPP-PA14, PAO1) and *Escherichia coli* strains were cultured on lysogeny broth (LB) agar or liquid media at 37C. LB was supplemented with gentamicin (50 μg/mL for *P. aeruginos*a, 30 μg/mL for *E. coli*) to maintain the

pHERD30T plasmid or carbenicillin (250 µg/mL for *P. aeruginosa*, 100 µg/mL for *E. coli*) to maintain pHERD20T or pMMBHE. To maintain pHERD30T and pMMBHE in the same strain of *P. aeruginosa*, double selection of 30 µg/mL gentamicin and 100 µg/mL carbenicillin was employed. In all *P. aeruginosa* experiments, expression from pHERD20/30T was induced with 0.1%

PAO1 SpyCas9 expression strain

SpyCas9 expressed from the P_{LAC} promoter of pUC18T-mini-Tn7T-Gm was integrated into the *P. aeruginosa* strain PAO1 chromosome by electroporation and Flp-mediated marker excision as previously described (Choi and Schweizer, 2006). To generate the heterologous Type II-A PAO1 strain the PAO1-attTn7::pUC18T-miniTn7T-P_{LAC}-SpyCas9 strain was transformed with pBAO72 (pMMB67HE-P_{LAC}-sgRNA) by electroporation. In all experiments with this strain, SpyCas9 and the sgRNA were induced with 1mM IPTG.

Construction of recombinant DMS3m$_{acr}$ phages

DMS3m$_{acrIF1}$ was generated as in (Bondy-Denomy et al., 2013) by infecting cells containing a recombination plasmid bearing JBD30 genes 34-38 (the anti-CRISPR locus with large flanking regions). JBD30 naturally carries *acrIF1* and has high genetic similarity to DMS3m$_{acrIE3}$, permitting for the selection of recombinant DMS3m phage which had acquired *acrIF1*. To generate the extended panel of DMS3m$_{acr}$ phages in this work, recombination cassettes were generated with regions from up and downstream the anti-CRISPR genes from JBD30 Gibson assembled to flank the *acr* gene of interest on pHERD20T or pHERD30T (see S1 for *acr* gene sources and exact details of *acr* locus architecture). Recombinant phages were generated by infecting cells bearing these recombination substrates. DMS3m$_{acr}$ phages were screened for their ability to resist CRISPR targeting, and the insertion of the anti-CRISPR gene was confirmed by PCR. Virulent derivatives of DMS3m$_{acr}$ phages were constructed by deleting gp1 (C repressor) using materials and methods from Cady et al., 2012.

Construction of DMS3m$_{acr\ gp52::GentR}$ phages

A recombination substrate with a gentamicin resistance cassette flanked by homology arms matching the DMS3m genome up and downstream of gp52 (450 bp and 260 bp, respectively) was assembled into pHERD20T using Gibson assembly. This recombination cassette was transformed into PA14 ΔCRISPR lysogenized with either DMS3m$_{acrIE3}$ or DMS3m$_{acrIF1}$.These transformed lysogens were grown under gentamicin selection for 16 h, then sub-cultured 1:100 into LB with gentamicin and 0.2 µg/mL mitomycin C to induce the DMS3m$_{acr}$ prophage. Supernatants were harvested after 24 hours of induction, and used to infect PA14 ΔCRISPR for 24 h. These cells were then plated on gentamicin plates to select for cells that had acquired a prophage bearing the gentamicin resistance cassette, and gentamicin resistant lysogens were then re-induced with 0.2 µg/mL mitomycin C to recover the recombinant phage.

Construction of DMS3m$_{acr\ gp1\text{-}JBD30}$ (Hybrid$_{acr}$) phages

DMS3m$_{acrIE3}$ and JBD30$_{acrIE3}$ were used to co-infect PA14 ΔCRISPR and the infected cells were mixed with molten top agar and poured onto solid plates. After 24 hours of growth at 30C, the phages were harvested by flooding the plate with SM buffer and collecting and clarifying the supernatant. Phages were then used to infect PA14 ΔCRISPR expressing the DMS3 C repressor from pHERD30T, and the infections were mixed with molten top agar and poured onto solid plates. After 24 hours of growth at 30 ºC, individual plaques with DMS3 morphology were picked, purified 3x by passage in PA14 ΔCRISPR and screened as shown in Figure S4B.

677
678 **Phage (PFU) quantification**
679 Phage plaque forming units (PFU) were quantified by mixed 10µl of phage at a with 150
680 µl of an overnight culture of host bacteria. The infection mixture was incubate at 37 ºC
681 for 10 minutes to promote phage adsorption, then mixed with 3 mLs molten top agar and
682 spread on an LB agar plate supplemented with 10 mM $MgSO_4$. After 16 hours of growth
683 30 ºC, PFUs were quantified.
684
685 **Phage titering**
686 A bacterial lawn was generated by spreading 3 mLs of top agar seeded with 150 µl of
687 host bacteria on a LB agar plate supplemented with 10 mM $MgSO_4$. 3 µl of phage
688 serially diluted in SM buffer was then spotted onto the lawn, and incubated at 30 ºC for
689 16 hours.
690
691 **Measurement of anti-CRISPR binding kinetics by surface plasmon resonance**
692 Purified Csy complex was covalently immobilized by amine coupling to the surface of a
693 carboxymethyldextran-modified (CM5) sensor chip. Purified 6his-tagged AcrIF4 was
694 injected into the buffer flow in increasing concentrations (1.85 nM, 55.6 nM, 167 nM, 500
695 nM, 1.5 uM), and Csy complex-AcrIF4 binding events were recorded in real time.
696 Experiments were conducted at 37°C, in 20 mM HEPES pH 7.5, 100 mM KCl, 1mM
697 TCEP, 0.005% Tween. Data were fit with a model describing Langmuir binding (i.e. 1:1
698 binding between free analyte and immobilized ligand). Kinetic rate constants were
699 calculated using Biacore evaluation software (GE).
700
701 **Liquid culture phage infections**
702 Liquid culture phage infections and growth curves were performed by infecting 140 µl of
703 *P. aeruginosa* 1:100 diluted overnights cultured in LB supplemented with 10 mM MgSO4
704 and antibiotics and inducer in a 96 well costar plate with 10 µl of phage diluted in SM
705 buffer. These infections proceeded for 24 hours in a BioTek Synergy microplate reader
706 at 37 ºC with continuous shaking. After 24 hours, phage was extracted treating each
707 sample with chloroform followed by centrifugation at 21,000 x g for 2 minutes.
708
709 **Lysogen acquisition and induction**
710 Overnight cultures of PA14 were subcultured at 1:100 for ~3 hours (OD_{600nm} = 0.3) in LB
711 supplemented with 10 mM MgSO4. 1 mL of cells were then infected with 10 µl DMS3m$_{acr}$
712 $_{gp52::GentR}$ and incubated for 50 minutes at 37 ºC, shaking at 100 rpm. The sample was
713 then treated with a 10% volume of 10X gentamicin, spun down at 8,000xg, and
714 resuspended in 200 ul of LB with 50 µg/mL gentamicin. 100 ul of sample was then plated
715 (after further dilution, if required) on gentamicin selection plates and incubated at 37 ºC.
716 To analyze the lysogens, the resulting colonies were grown for 16 hours in LB + 10 mM
717 MgSO4 (no selection), the supernatants harvested, and serial dilutions spotted onto a
718 lawn of PA14 ΔCRISPR. Crude genomic DNA for PCR analysis was harvested from the
719 lysogens by boiling 10 µl of culture in 0.02% SDS for 10 minutes.
720
721 **Lysogen PCR**
722 PCR amplification of 2 µl of crude genomic DNA harvested from lysogens was used to
723 screen for the presence of *DMS3m-gp52* and *gentR* using MyTaq (Bioline) polymerase
724 with MyTaq GC buffer under standard conditions.
725

Figure 1

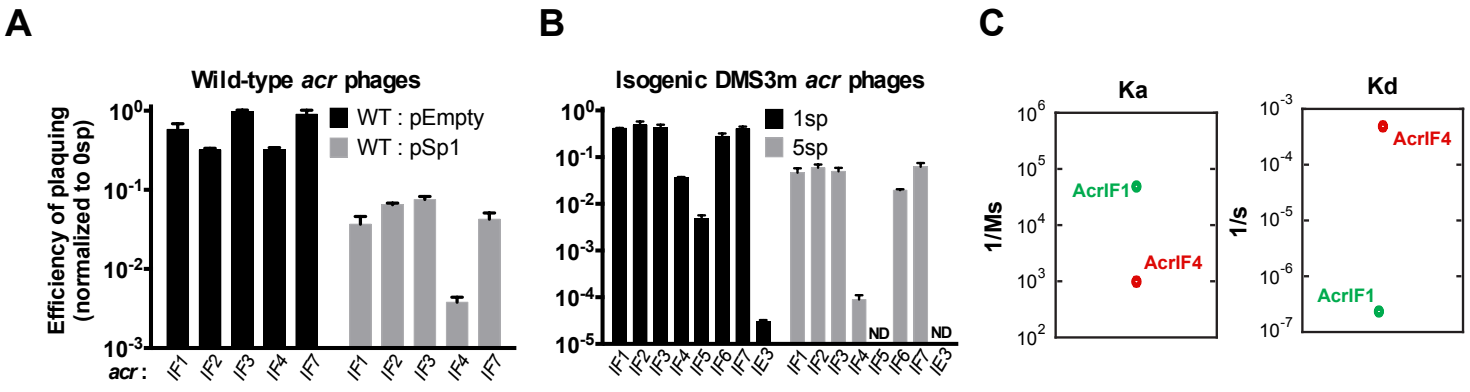

Figure 2

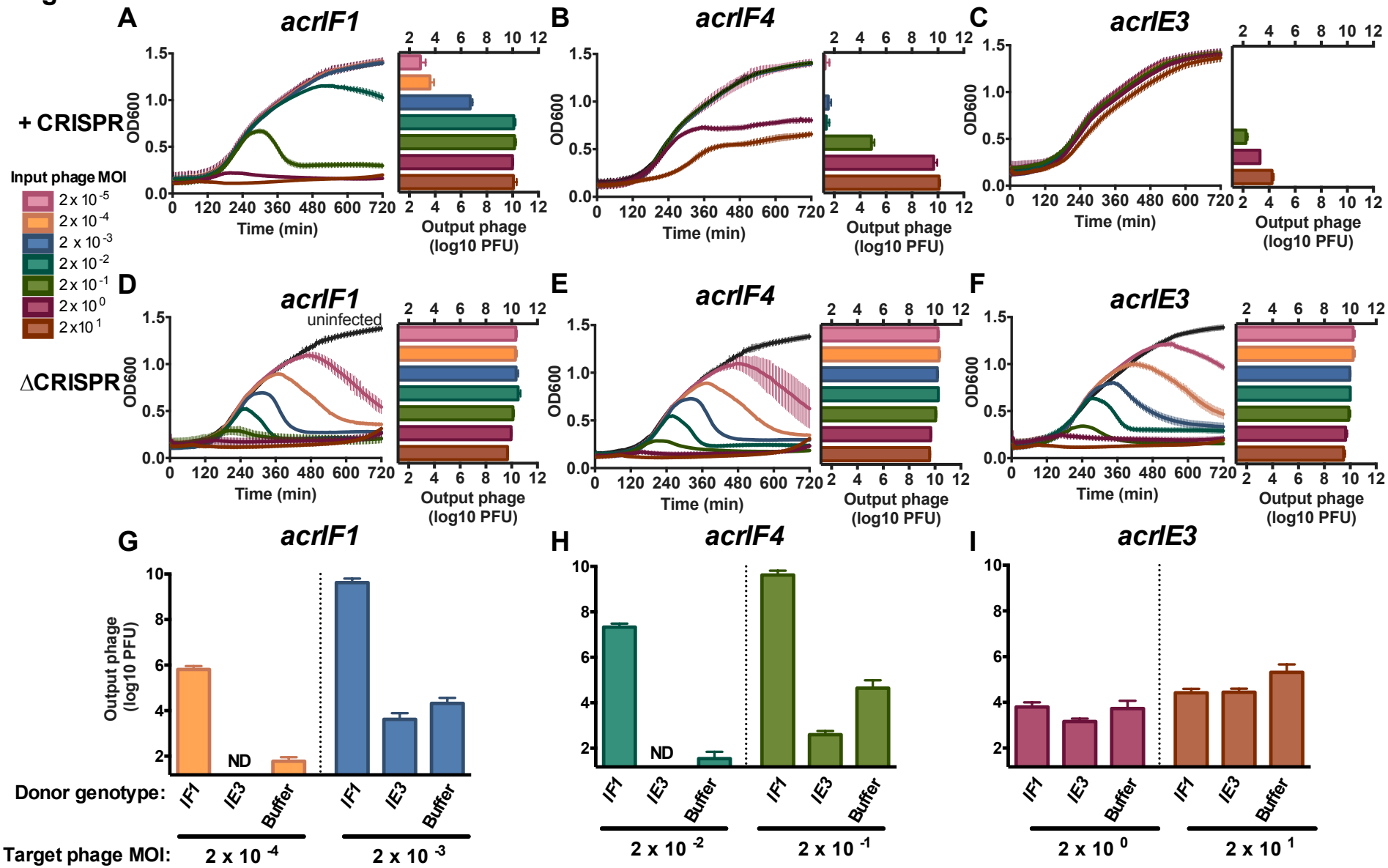

Figure 3

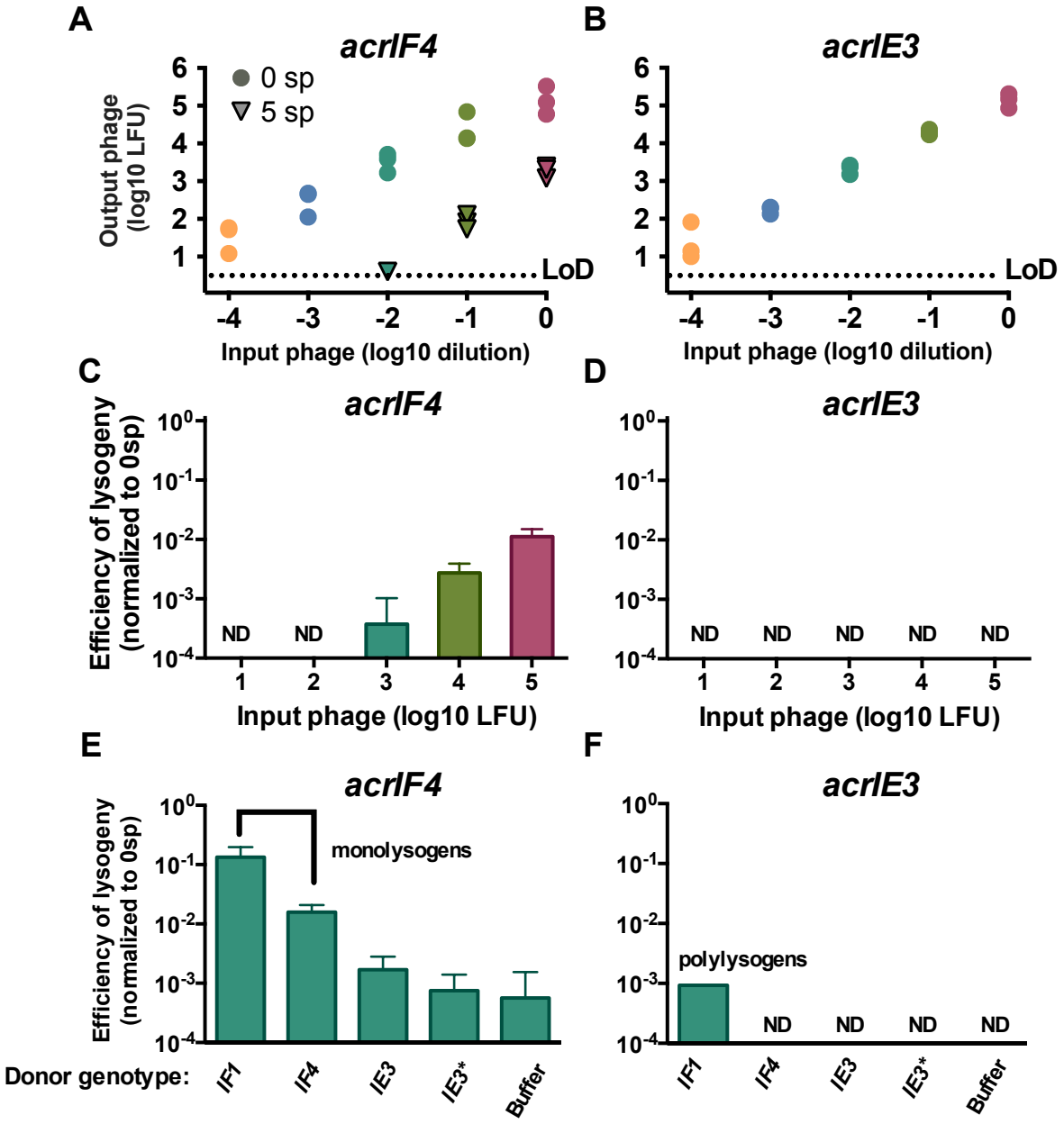

Figure 4

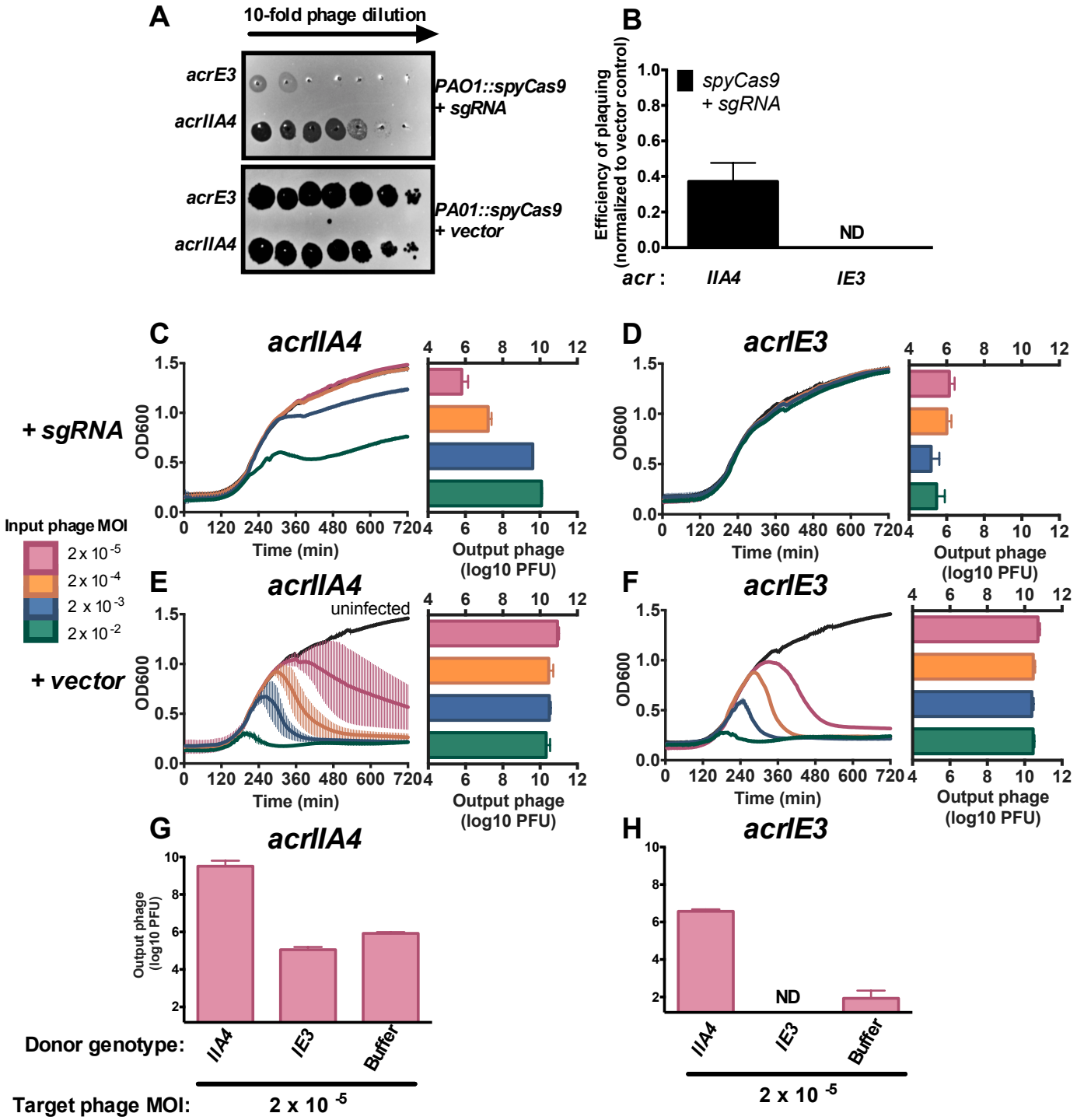

Figure 5

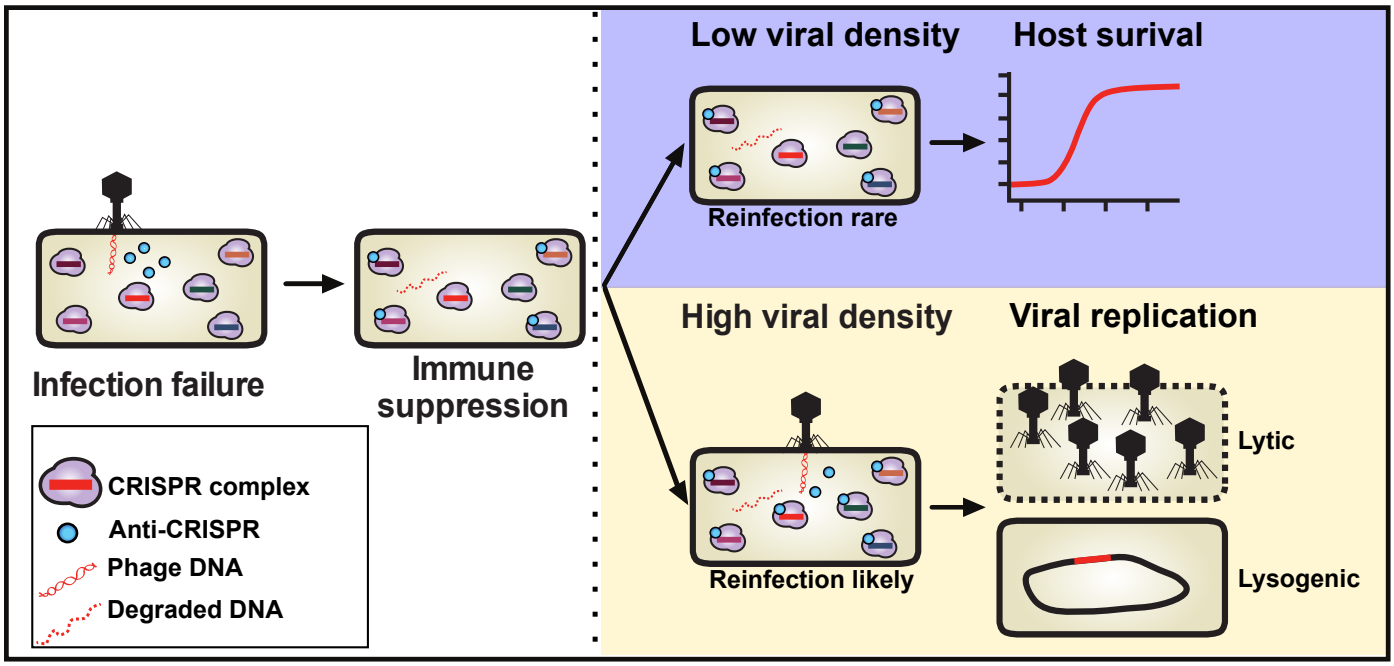

Supplementary Figure 1

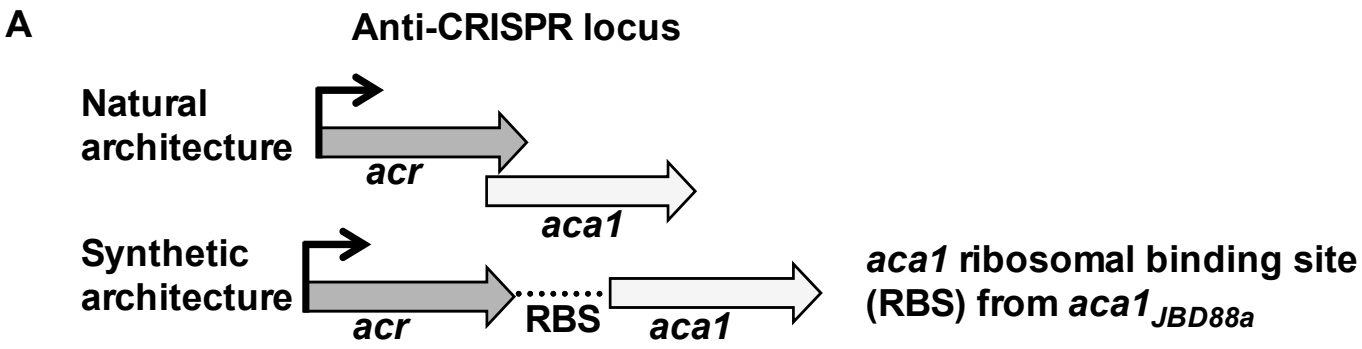

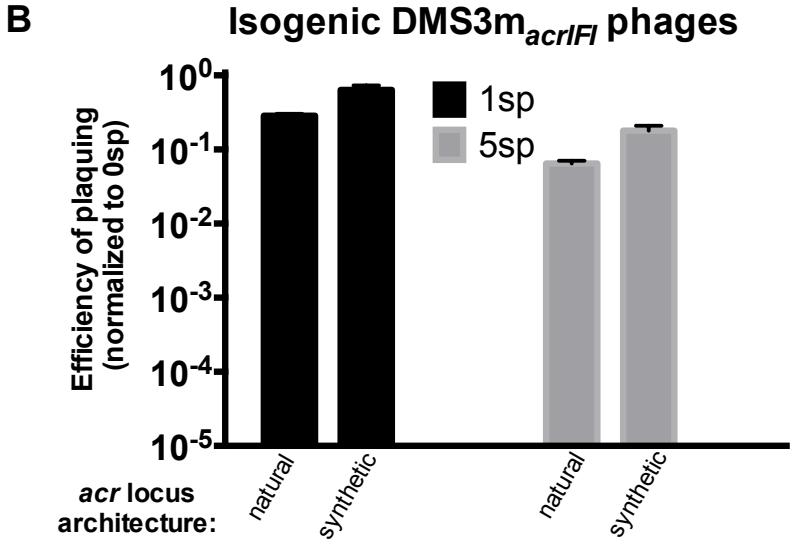

C DMS3m$_{acr}$ phages

Phage	DMS3m$_{acr}$ architecture	*acr* gene source	Acr Accession
DMS3m$_{acrIE3}$ (parent phage, no manipulation)	natural	DMS3m (gp30)	WP_003723290.1
DMS3m$_{acrIF1}$	natural	JBD30 (gp35)	YP_007392342.1
DMS3m$_{acrIF2}$	natural	MP29 (gp29)	YP_002332454.1
DMS3m$_{acrIF3}$	natural	JBD88a (gp33)	YP_007392440.1
DMS3m$_{acrIF4}$	natural	JBD26 (gp37)	WP_016068584.1
DMS3m$_{acrIF5}$	synthetic	JBD5 (gp36)	YP_007392740.1
DMS3m$_{acrIF6}$	synthetic	*Pseudomonas aeruginosa* strain PSE05 (prophage)	WP_043884810.1
DMS3m$_{acrIF7}$	natural	LPB1 (gp29)	YP_009146150.1
DMS3m$_{acrIIA4}$	synthetic	*Listeria monocytogenes* J0161 (prophage)	WP_003723290.1

Supplementary Figure 2

A

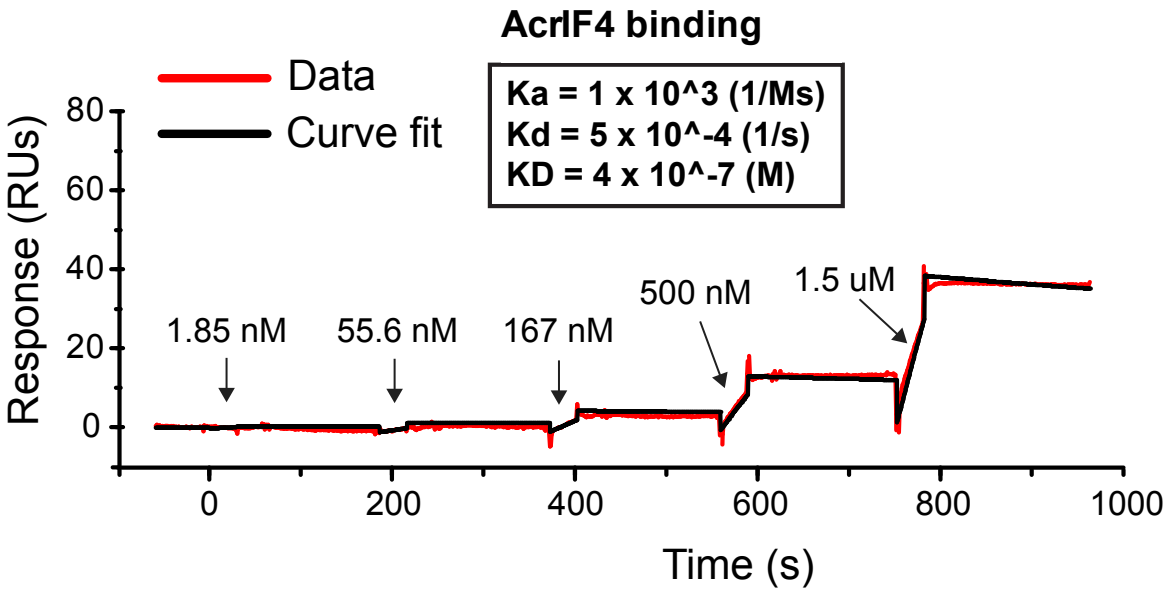

Supplementary Figure 3

A

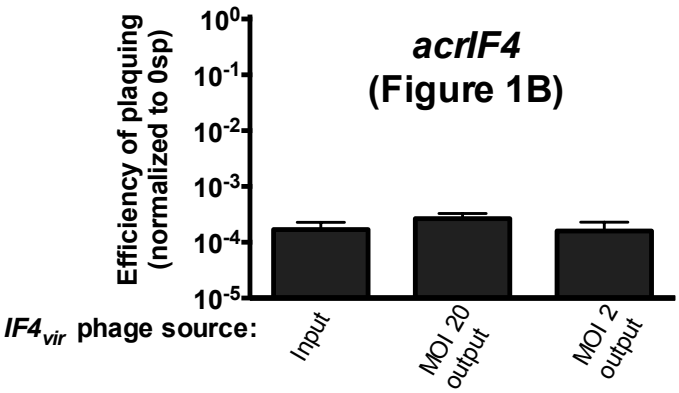

Supplementary Figure 4

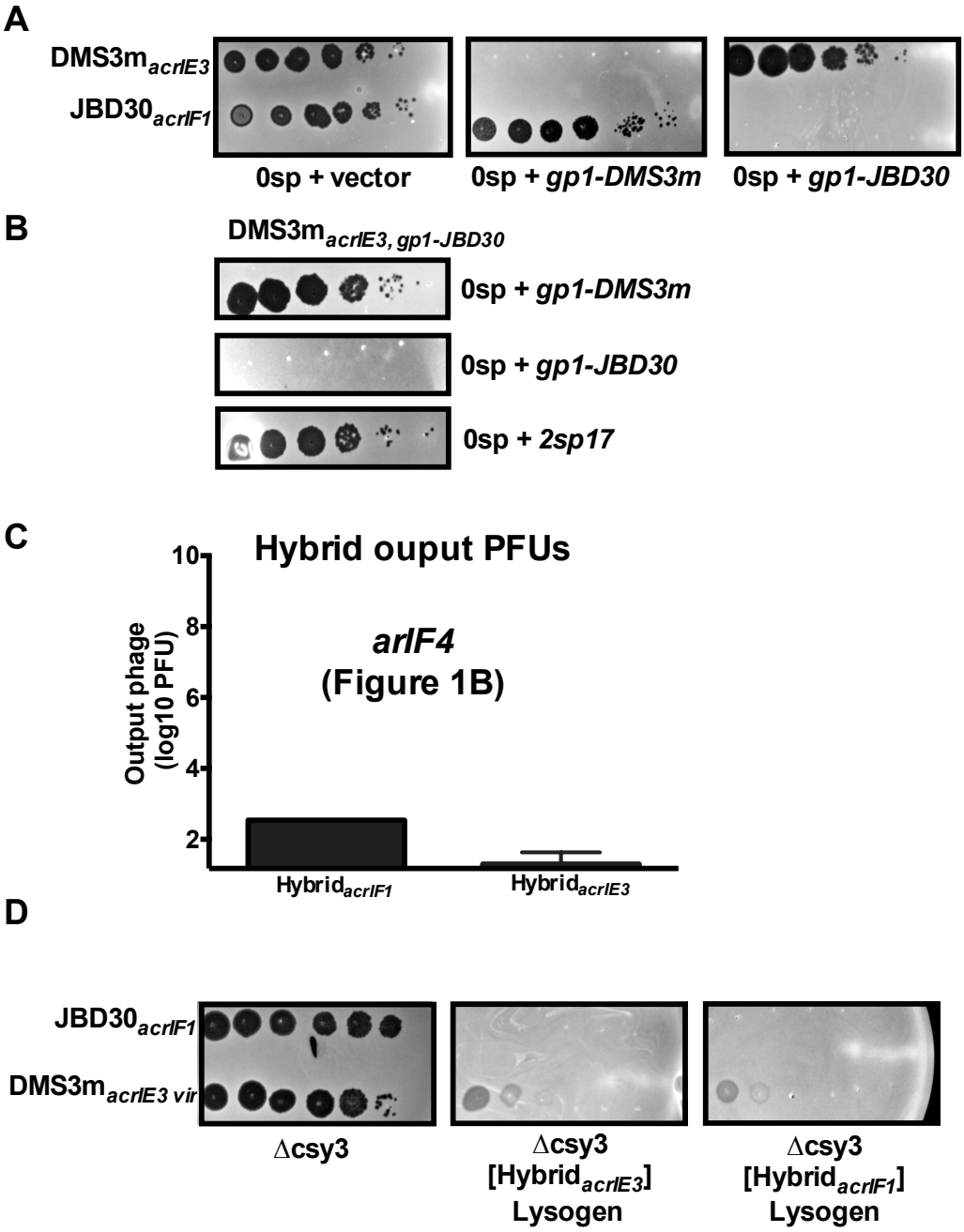

Supplementary Figure 5

A

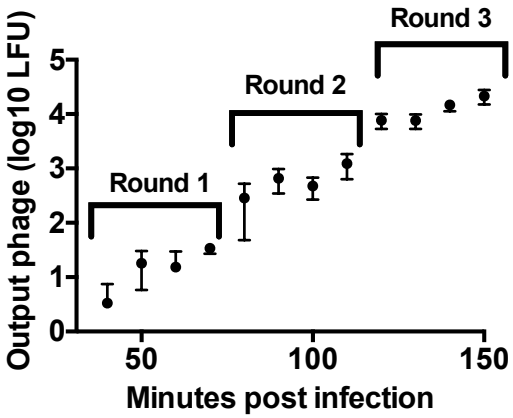

Supplementary Figure 6